Small separations and phase shift differences of l = 0, 1 p-modes

Ian W. Roxburgh

A&A 493, 185–191 (2009)
DOI: 10.1051/0004-6361:200811047

Astronomy & Astrophysics

Small separations and phase shift differences of $\ell = 0, 1$ p-modes

I. W. Roxburgh[1,2]

[1] Astronomy Unit, Queen Mary, University of London, Mile End Road, London E1 4NS, UK
e-mail: I.W.Roxburgh@qmul.ac.uk
[2] LESIA, Observatoire de Paris, Place Jules Janssen, 92195 Meudon, France

Received 27 September 2008 / Accepted 26 October 2008

ABSTRACT

Aims. We investigate the diagnostic potential of $\ell = 0, 1$ p-modes and the origin of the periodicity in their small separations.
Methods. We used theoretical analysis, phase-shifts, modelling. and data analysis.
Results. The periodicity in the small separations between modes of $\ell = 0, 1$ is determined by the acoustic *radius* of the base of the outer convective envelope. The mean variation is determined primarily by the structure of the inner core. The separations are related to the inner phase shifts differences $\delta_1 - \delta_0$ which we show can be determined directly from the frequencies. The modulation period is shifted slightly by the frequency dependence of the phase shifts and the amplitudes. We present results using data from the BiSON, IRIS, and GOLF experiments, and a solar model, all of which give a modulation period of $\sim 359 \pm 5$ μHz corresponding to an acoustic radius $\sim 1422 \pm 20$ s.

Key words. stars: oscillations – stars: interiors

1. Introduction

The small separations $d_{\ell,\ell+2} = \nu_{n,\ell} - \nu_{n-1,\ell+2}$ between p-modes of oscillation have been widely used as diagnostics of the solar and stellar interiors (cf. Gough 1983; Provost 1984; Christensen-Dalsgaard 1984, 1988; Ulrich 1986), as they are primarily determined by the interior structure of the star (cf. Tassoul 1980). Since the predicted amplitudes of modes of degree $\ell = 0, 1$ are considerably larger than those of $\ell = 2, 3$, for some stars these may be the only modes that can be reliably determined and the only small separations available being those between modes with $\ell = 0, 1$ defined as (cf. Roxburgh 1993)

$$d_{01} = \nu_{n,0} - (\nu_{n-1,1} + \nu_{n,1})/2, \quad d_{10} = (\nu_{n,0} + \nu_{n+1,0})/2 - \nu_{n,1}. \quad (1)$$

The diagnostic value of these separations is explored in the present paper.

Figure 1a shows the separations d_{01}, d_{10} multiplied by $\nu^* = \nu/(2500\ \mu\text{Hz})$ for a solar modelA (a smoothed version of model S, Christensen-Dalsgaard et al. 1996); they display a periodic modulation about a mean curve which is not present in the d_{02} separations (Fig. 1c). The periodicity is clearer in Fig. 1b which plots the 5 point differences (Roxburgh & Vorontsov 2003a). (Hereafter R&V = Roxburgh & Vorontsov.)

$$dd_{01} = \frac{1}{8}(\nu_{n-1,0} - 4\nu_{n-1,1} + 6\nu_{n,0} - 4\nu_{n,1} + \nu_{n+1,0}) \quad (2)$$

$$dd_{10} = -\frac{1}{8}(\nu_{n-1,1} - 4\nu_{n,0} + 6\nu_{n,1} - 4\nu_{n+1,0} + \nu_{n+1,1}). \quad (3)$$

We show below that the modulation period is determined by the acoustic radius of the base of the convective envelope, whilst the mean curve which is similar to, but different from, that of d_{02}, is determined by the structure of the deep interior and therefore provides a diagnostic of the inner structure.

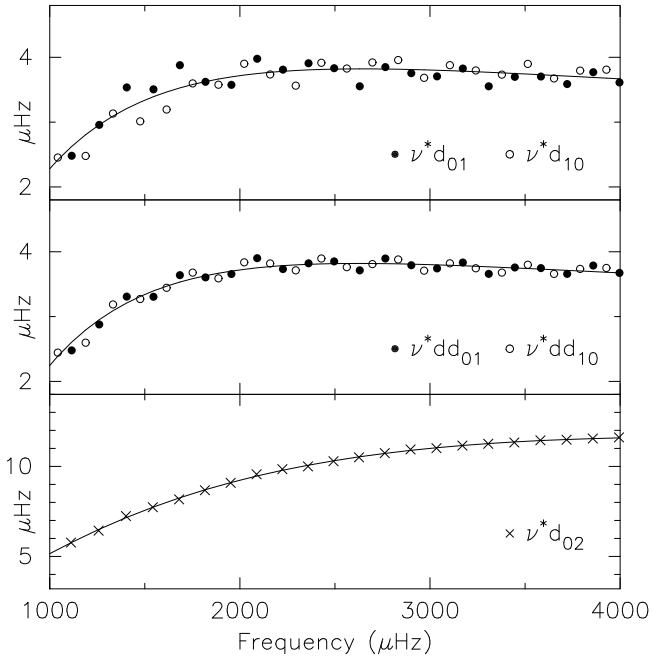

Fig. 1. *Top panel*: $\nu^* d_{01}, \nu^* d_{10}$; *middle panel*: $\nu^* dd_{01}, \nu^* dd_{10}$, *bottom panel*: $\nu^* d_{02}$, for solar model A. $\nu^* = \nu$ in units of 2500 μHz.

2. Solar data

Figure 2 shows the small separations $\nu^* dd_{01}, \nu^* dd_{10}$ for 3 solar data sets from the ground based experiments BiSON and IRIS and the GOLF instrument on SOHO. The BiSON data set was for the time span 1993–2003 (Chaplin et al. 2007; Verner 2008); the IRIS data set for 1989–99 (Fossat et al. 2003) and the P3 GOLF data set for 1996–1999 (Gelly et al. 2002). All show the same periodicity and phase. These data are analysed in more detail in Sect. 8 below.

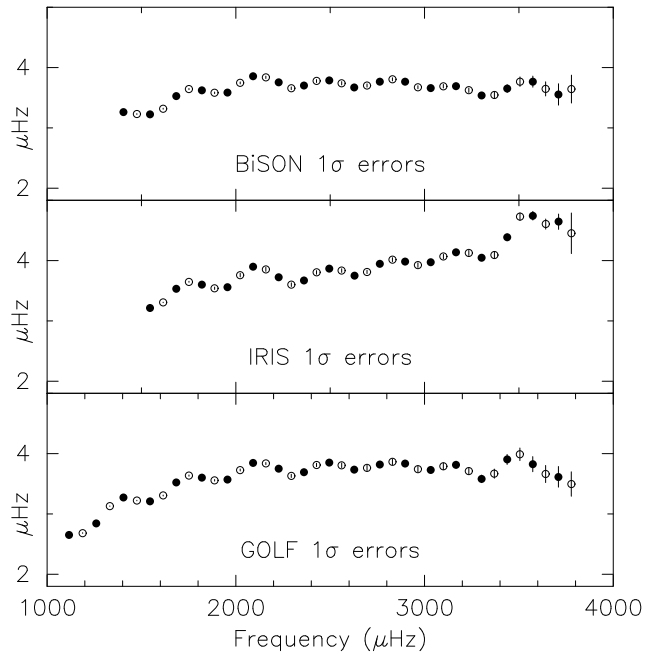

Fig. 2. Variation of small separations $\nu^* dd_{01}, \nu^* dd_{10}$ with ν for frequencies obtained by the BiSON, IRIS and GOLF experiments. All data sets show the same periodicity and the same phase.

3. Determination of the modulation period

Inspection of Figs. 1a and b gives a modulation period of ≈350 μHz. A more quantitative estimate is obtained by fitting a low order curve to remove the trend (as shown in Figs. 1a,b) and taking the Fourier transform of the residuals. The trend was removed by a least squares fit to the function

$$F(\nu) = \sum_{k=0}^{N} \frac{C_k}{(\nu + \nu_0)^k} \quad \text{with} \quad \nu_0 = 2500\,\mu\text{Hz}, \quad N = 3. \tag{4}$$

Figure 3a gives the residuals for $\nu^* d_{01}, \nu^* d_{10}$ and Fig. 3b the residuals for $\nu^* dd_{01}, \nu^* dd_{10}$. Figures 4a,b give the corresponding Fourier power spectra (amplitude^2). Both power spectra have a peak at ∼359 μHz. As shown below, this modulation is caused by the region of sharp change in the structure at, and just below, the base of the convective envelope, and has a period of approximately $1/(2t_1)$ where t_1 is the acoustic *radius* of the base of the envelope. The secondary peak at 166 μHz in Fig. 4a corresponds to the acoustic *radius* of the HeII ionisation layer, whereas the other peak is due to the large separations; these are suppressed by the 5 point differences dd.

4. Cause of the periodic modulation

As is well known, simple asymptotic analysis shows that discontinuities and steep gradients in the acoustic structure of a star induce periodic modulations in the frequencies with period $1/(2\tau_1)$ where τ_1 is the acoustic depth of the region of rapid variation (Vorontsov 1988; Gough 1990; R&V 1994b; Monteiro et al. 1994). Likewise such discontinuities induce periodic variations with period $1/(2t_1)$ where t_1 is the acoustic radius, the two being just alternative representations of each other (R&V 2001). Further details are given in Sect. 7 below. The acoustic radius t and acoustic depth τ are defined by

$$t = \int_0^r \frac{\mathrm{d}r}{c}, \quad \tau = \int_r^R \frac{\mathrm{d}r}{c} \tag{5}$$

where $c(r)$ is the sound speed ($c^2 = \Gamma_1 P/\rho$).

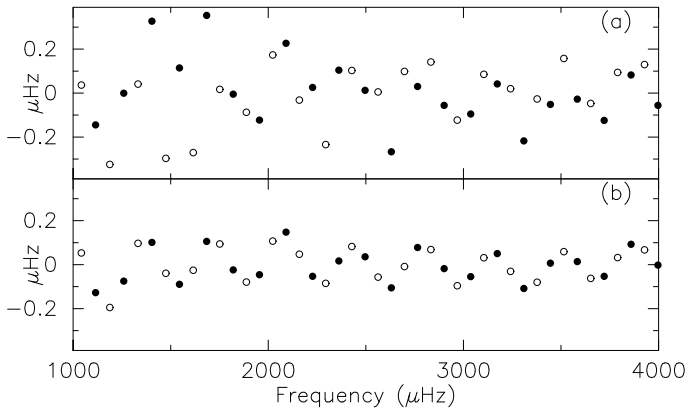

Fig. 3. Residuals to a low order fit; **a)** $\nu^* d_{01}, \nu^* d_{10}$, **b)** $\nu^* dd_{01}, \nu^* dd_{10}$.

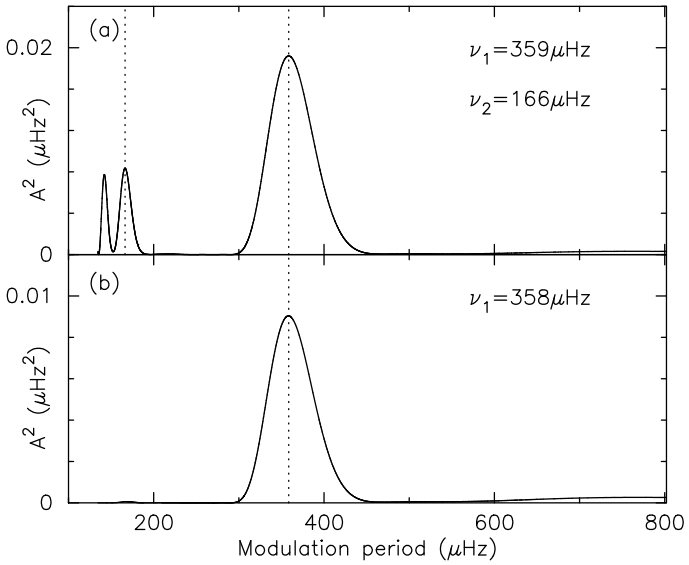

Fig. 4. Power spectra of the residuals: **a)** $\nu^* d_{01}, \nu^* d_{10}$, **b)** $\nu^* dd_{01}, \nu^* dd_{10}$.

For model A used in the calculations for Figs. 3a and b, the base of the convective zone is at an acoustic radius of $t = 1422$ s or equivalently an acoustic depth of $\tau = 2171$ s; so the equivalent modulation periods are 352 μHz and 230 μHz. Also in model A the location of the region of rapid change in acoustic variables due to HeII ionisation is around $t \sim 3000$ s, $\tau \sim 600$ s, and the corresponding modulation periods are ∼167 μHz and ∼833 μHz.

It is clear from Figs. 4a and b that the signal in the separations with a modulation period of ∼359 μHz corresponds to the acoustic radius of the region at the base of the convective zone, not the acoustic depth. The fact that the peaks are at ∼359 μHz rather than 352 μHz is due to two factors: a) the acoustic waves are not pure sine waves but are subject to a frequency dependent phase shift; b) the amplitudes of the contributions to the oscillating component are frequency dependent; both contribute to the Fourier transform shifting the peak from 352 to 359 μHz. Details of the various contributions to the oscillating component and the frequency shift are given in Sect. 7 below.

5. Small separations and phaseshifts

As shown by R&V (2000, 2003a,b), by matching the solution of the oscillation equations in the inner and outer layers at some intermediate acoustic radius t_f, the adiabatic oscillation

eigenfrequencies $\nu_{n,\ell}$ of a spherical star necessarily satisfy the *Eigenfrequency equation*

$$2\pi\nu_{n,\ell}T = \pi\left(n + \frac{\ell}{2}\right) + \alpha_\ell(\nu,\tau_f) - \delta_\ell(\nu,t_f) \quad \text{integer } n \tag{6}$$

where the *inner phase shifts* δ_ℓ and *outer phase shifts* α_ℓ are defined in terms of the variable

$$\psi_\ell = rp'_\ell/(\rho c)^{1/2} \tag{7}$$

as

$$\chi_\ell = \frac{2\pi\nu\psi_\ell}{\mathrm{d}\psi_\ell/\mathrm{d}t} = \tan\left[2\pi\nu t - \frac{\pi}{2}\ell + \delta_\ell(\nu,t)\right], \quad t \le t_f \tag{8}$$

$$\chi_\ell = -\frac{2\pi\nu\psi_\ell}{\mathrm{d}\psi_\ell/\mathrm{d}\tau} = -\tan\left[2\pi\nu\tau - \alpha_\ell(\nu,\tau)\right], \quad \tau = T - t \le \tau_f. \tag{9}$$

Here p'_ℓ is the Eulerian pressure perturbation for a mode of degree ℓ, t, τ the acoustic radius and depth as defined in Eq. (5), and $T = t(R)$ is the acoustic radius of the star or, more precisely, the radius at which the boundary conditions are imposed (here approximately at an optical depth of 10^{-4}). The term $\pi\ell/2$ in Eq. (8) is included to allow for the spherical Bessel function character of the solution for ψ (cf. R&V 1994a).

The inner and outer phase shifts $\delta_\ell(\nu), \alpha_\ell(\nu)$ as defined in Eqs. (8) and (9) are continuous functions of frequency. For any frequency they are given by *partial wave* solutions of the oscillations equations (cf. R&V 2000): for δ these are solutions which are regular at the centre and satisfy the the surface gravitational boundary conditions; for α they are solutions which satisfy the surface boundary conditions. For modes of degree $\ell = 0, 1$ this completely determines $\alpha_\ell(\nu)$ since for $\ell = 0$ the equations reduce to second order and the oscillating gravitational potential and its derivative ϕ', $\mathrm{d}\phi'/\mathrm{d}r$ do not contribute to the determination of ψ, whereas for $\ell = 1$ modes ϕ', $\mathrm{d}\phi'/\mathrm{d}r = 0$ at the surface as the external gravitational dipole moment is identically zero for $\ell = 1$ modes. The Eigenfrequency Eq. (6) is then given by demanding continuity between the inner and outer solutions at some $t = t_f$ which gives the discrete eigenfrequencies $\nu_{n,\ell}$.

The partial waves and eigenfrequencies can always be represented as in Eqs. (6)–(9); the value of this representation is that, with the above definition of ψ_ℓ (Eq. (7)) both α_ℓ, δ_ℓ are almost independent of t_f in the intermediate layers of a star (cf. R&V 1996) and α_ℓ is almost independent of ℓ. α_ℓ is therefore determined by the structure of the outer layers ($t \ge t_f$) and δ_ℓ by the structure of the inner layers ($t \le t_f$).

Figure 5a shows the variation of α and δ with acoustic radius for $\nu = 2500\,\mu$Hz for model A; Fig. 5b shows their variation with frequency evaluated at $x = x_f = 0.9$; whilst Fig. 5c shows the variation with frequency of the differences $\alpha_1 - \alpha_0$ and $\delta_1 - \delta_0$. As stated above $\alpha_1 \approx \alpha_0$. The difference $\delta_1 - \delta_0$ displays the periodic variation with modulation period ~359 μHz, caused by the base of the convective envelope.

Using the eigenfrequency Eq. (6), taking α_ℓ to be independent of ℓ, and α, δ_ℓ as continuous functions of ν, the small separations d_{01}, d_{10} can be expressed as

$$d_{01} = \frac{1}{2\pi T}\left(\delta_1 - \delta_0 - \frac{\mathrm{d}^2(\alpha - \delta_1)}{\mathrm{d}\nu^2}\frac{\Delta_1^2}{8} + \ldots\right), \quad \nu = \nu_{n,0} \tag{10}$$

$$d_{10} = \frac{1}{2\pi T}\left(\delta_1 - \delta_0 + \frac{\mathrm{d}^2(\alpha - \delta_0)}{\mathrm{d}\nu^2}\frac{\Delta_0^2}{8} + \ldots\right), \quad \nu = \nu_{n,1} \tag{11}$$

with large separations $\Delta_1 = \nu_{1,n} - \nu_{n-1,1}$, $\Delta_0 = \nu_{n+1,0} - \nu_{n,0}$.

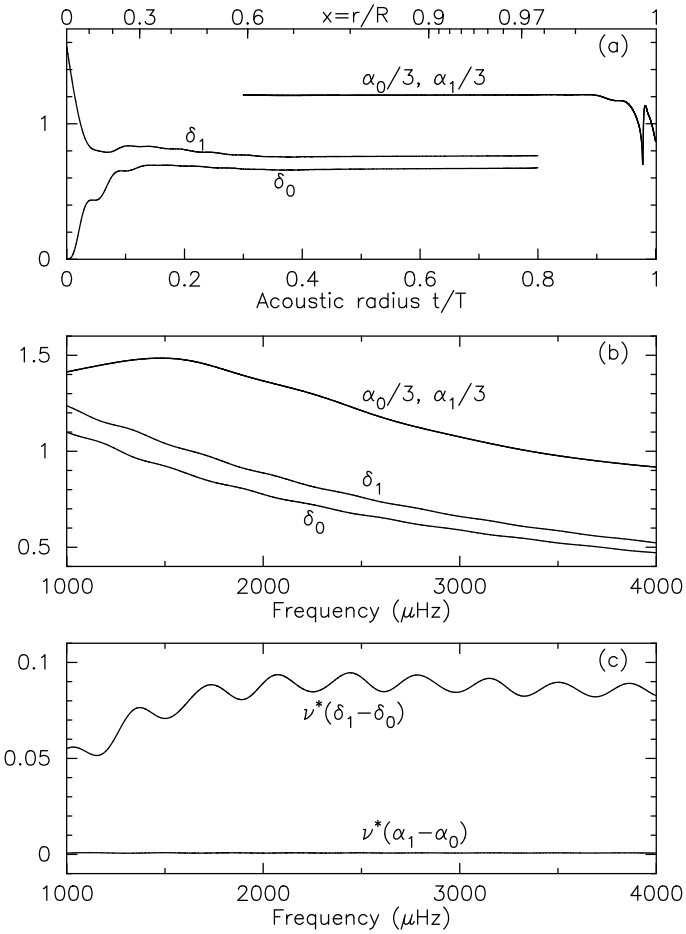

Fig. 5. Phase shifts δ_0, δ_1 and α_0, α_1 for model A: **a)** variation with acoustic radius for $\nu = 2500\,\mu$Hz. α_0, α_1 cannot be separated in these figures; **b)** variation with frequency for $x_f = 0.9, t_f/T = 0.615$; **c)** variation of $\nu^*(\delta_1 - \delta_0)$ and $\alpha_1 - \alpha_0$ with frequency.

The surface phase shift α, which has within it the modulation from the HeII ionisation zone, contributes to the small separations, this produces the considerable scatter in the residuals plotted in Fig. 3a. However since

$$dd_{01}(n) = \frac{1}{2}d_{01}(n) + \frac{1}{4}\left(d_{10}(n) + d_{10}(n-1)\right) \tag{12}$$

the contributions from $\mathrm{d}^2\alpha/\mathrm{d}\nu^2$ to dd_{01} almost cancel out, but the contribution from $\mathrm{d}^2(\delta_1 - \delta_0)/\mathrm{d}\nu^2$ is of the same sign as $\delta_1 - \delta_0$, which reduces the amplitude of the periodic variation in dd_{01}, and similarly that of dd_{10}.

6. Determination of the inner phase shift difference $\delta_1 - \delta_0$

Since the small separations are governed by the phase shift difference we here show how to determine this difference directly from the frequencies. We write the Eigenfrequency Eq. (6) in the form

$$\alpha_\ell(\nu_{n,\ell}) - \delta_\ell(\nu_{n,\ell}) = 2\pi\nu_{n,\ell}T - \pi\left(n + \frac{\ell}{2}\right). \tag{13}$$

The value of the acoustic radius of the star T is unknown, it is a theoretical construct which depends on where the astrophysicist imposes boundary conditions in their analysis, but it is of the

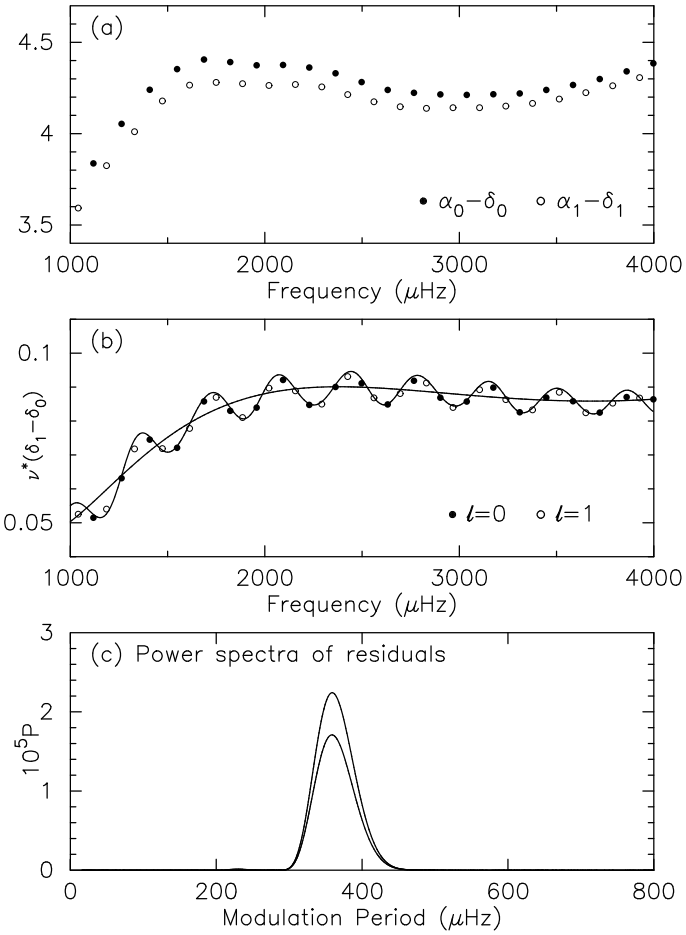

Fig. 6. a) $\alpha-\delta$ as determined from the frequencies and Eigen-frequency Eq. (14) with $\Delta_0 = 136\ \mu$Hz. **b)** Phase shift difference $\nu^*(\delta_1 - \delta_0)$ determined from the eigenfrequencies by interpolation (points), the model values (continuous periodic line), the mean variation (smooth line). **c)** Power spectra of residuals to mean variation – the smaller maximum is that obtained using the points determined from the frequencies.

order of $1/(2\Delta_0)$ where Δ_0 is some typical value of the large separations ($\Delta_{n,\ell} = \nu_{n+1,\ell} - \nu_{n,\ell}$). We first rewrite Eq. (12) as

$$\alpha^*_\ell(\nu_{n,\ell}) - \delta_\ell(\nu_{n,\ell}) = \pi\,\frac{\nu_{n,\ell}}{\Delta_0} - \pi\left(n + \frac{\ell}{2}\right) \tag{14}$$

where

$$\alpha^*_\ell = \alpha_\ell + \pi\left(\frac{1}{\Delta_0} - 2T\right)\nu_{n,\ell}. \tag{15}$$

From here on we drop the asterisk from α^*. Taking a value of $\Delta_0 = 136\ \mu$Hz the functions $\alpha_\ell - \delta_\ell$ are plotted in Fig. 6a.

We now draw on theoretical analysis that α_ℓ is essentially independent of ℓ (Fig. 5c) and that both α and δ_ℓ can be considered as continuous functions which vary on a scale sufficiently large for us to be able to interpolate between the points determined by the frequencies. This enables us to subtract the two curves to determine the values of $\delta_1 - \delta_0$. The points in Fig. 6b show the resulting values of $\delta_1 - \delta_0$ at the eigenfrequencies $\nu_{n,\ell}$ obtained using cubic spline interpolation. Note that these values are independent of the choice of mean large separation Δ_0 and T since the addition to α_ℓ in Eq. (15) cancels out in the subtraction. The solid curve is the value obtained from solving the oscillation equations for partial waves and calculating the inner phase shifts δ_ℓ at $x_f = 0.9$ as illustrated in Fig. 5c. I emphasise that the points displayed in Fig. 6b are obtained from the frequencies alone. The small differences between the points and the continuous curve are due to several factors: a) interpolation is not exact; b) $\alpha_1(\nu)$ is not exactly equal to $\alpha_0(\nu)$; c) the $\delta_\ell(\nu)$ are not exactly constant in the outer layers. Nevertheless the agreement is good. Panel (c) shows the power spectra of the residuals to a low order fit as in Eq. (5). The amplitude derived from the points in Fig. 6b is somewhat less than that derived from the continuous model values, but the location of the maxima are almost the same at ~359 μHz.

In Sect. 8 below this analysis is applied to data from the BiSON. IRIS and GOLF experiments.

7. Theory of the inner phaseshifts

The equations governing the Eulerian pressure perturbation p', gravitational potential perturbation ϕ' and radial displacement ξ for an oscillation with angular frequency $\omega = 2\pi\nu$ are (cf. Unno et al. 1979)

$$\frac{\mathrm{d}\xi}{\mathrm{d}r} + \frac{2}{r}\xi - \frac{g}{c^2}\xi + \left(1 - \frac{\ell(\ell+1)c^2}{\omega^2 r^2}\right)\frac{p'}{\rho c^2} - \frac{\ell(\ell+1)}{\omega^2 r^2}\phi' = 0 \tag{16}$$

$$\frac{\mathrm{d}p'}{\mathrm{d}r} + \frac{g}{c^2}p' - (\omega^2 + 4\pi G\rho - N^2)\rho\xi + \rho\chi = 0 \tag{17}$$

$$\frac{\mathrm{d}\phi'}{\mathrm{d}r} = \chi - 4\pi G\rho\xi \tag{18}$$

$$\frac{\mathrm{d}\chi}{\mathrm{d}r} = 4\pi G\frac{\ell(\ell+1)}{\omega^2 r^2}p' + \frac{\ell(\ell+1)}{r^2}\left(1 + \frac{4\pi G\rho}{\omega^2}\right)\phi' - \frac{2}{r}\chi. \tag{19}$$

For $\ell = 0$ modes, χ is identically zero and the solution for ξ, p' are independent of ϕ'. For $\ell = 1$ modes both ϕ' and χ are zero at the surface (since there is no external gravitational moment for dipole oscillations), and both remain very small in the bulk of the star but are important in the central regions. Since we are interested in the region near and above the base of the convective zone we can, to a reasonable approximation, neglect ϕ' and χ in the above equations which then reduce to a second order system. (This is not quite the Cowling approximation since it is χ we are neglecting not $\mathrm{d}\phi'/\mathrm{d}r$, this gives the exact solution for $\ell = 0$.)

The equation governing the variable $\psi_\ell = rp'_\ell/(\rho c)^{1/2}$ (Eq. (7)) can then be reduced to one second order equation with acoustic radius $t = \int \mathrm{d}r/c$ as independent variable namely

$$\frac{\mathrm{d}^2\psi_\ell}{\mathrm{d}t^2} - Q\frac{\mathrm{d}\psi_\ell}{\mathrm{d}t} + \left[\omega^2 - V_\ell\right]\psi_\ell = 0 \tag{20}$$

where

$$\begin{aligned} V_\ell &= U_0 + \ell(\ell+1)U_2,\ U_0 = A^2 + QA - \frac{\mathrm{d}A}{\mathrm{d}t} + N^2 - 4\pi G\rho \\ A &= \frac{c}{4\Gamma_1}\frac{\mathrm{d}\Gamma_1}{\mathrm{d}r} - \frac{cN^2}{4g} + \left(\frac{3-\Gamma_1}{4}\right)\frac{g}{c} - \frac{c}{r} = \frac{1}{2}\frac{\mathrm{d}}{\mathrm{d}t}\left(\log\left[\frac{\rho c}{r^2}\right]\right) + \frac{g}{c} \\ U_2 &= F\frac{c^2}{r^2},\ Q = \frac{1}{F}\frac{\mathrm{d}F}{\mathrm{d}t},\ F = 1 + \frac{4\pi G\rho}{\omega^2} - \frac{N^2}{\omega^2}. \end{aligned} \tag{21}$$

This can be further reduced to a first order equation in the variable $\chi = \omega\psi_\ell/(\mathrm{d}\psi_\ell/\mathrm{d}t)$ (cf. Eq. (8))

$$\omega\frac{\mathrm{d}\chi_\ell}{\mathrm{d}t} - \omega^2 + Q\,\omega\chi_\ell - (\omega^2 - V_\ell)\chi_\ell^2 = 0. \tag{22}$$

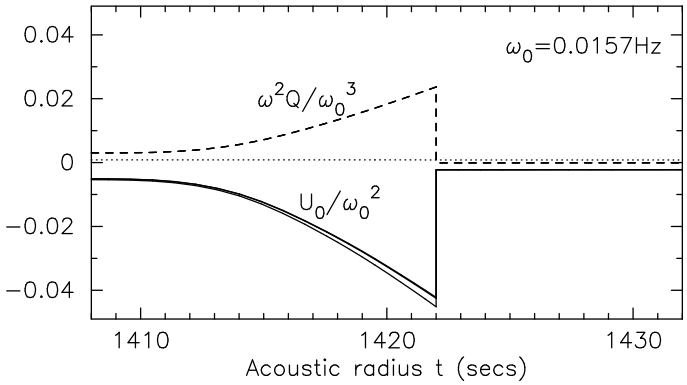

Fig. 7. Acoustic potentials at base of the convective zone: U_0/ω_0^2 (solid lines), $\omega^2 Q/\omega_0^3$ (dashed lines), and U_2/ω_0^2 (fine dotted lines), at a frequencies $\nu = 1000, 2500, 4000\ \mu$Hz.

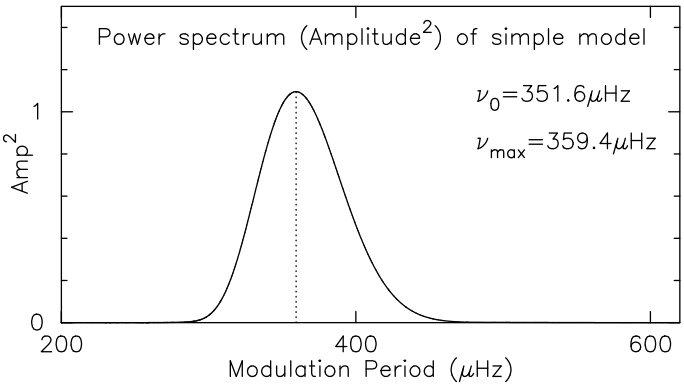

Fig. 8. Power spectrum (Ampliude^2) of simple model Eq. (28). The modulation period corresponding to the base of the convective zone is $\nu_0 = 352\ \mu$Hz but the maximum power is shifted to 359 μHz due to the frequency dependency of the phase shifts δ_0, δ_1 and of the amplitudes of the two components.

Setting $\chi_\ell = \tan(\omega t + \delta_\ell - \ell\pi/2)$ (cf. Eq. (8)) we obtain the equation for the internal phase shifts δ_ℓ as

$$\frac{\mathrm{d}\delta_\ell}{\mathrm{d}t} = -\frac{V_\ell}{\omega}\sin^2(\omega t+\delta_\ell-\ell\pi/2)-\frac{Q}{2}\sin(2[\omega t+\delta_\ell-\ell\pi/2]). \quad (23)$$

For $\ell = 0$ this equation is valid throughout the star and can therefore be integrated, subject to $\delta_0 = 0$ at $t = 0$ to give $\delta_0(t, \omega)$. For $\ell = 1$ one must include the gravitational potential perturbation ϕ' in the central regions of the star, and then Eq. (23) can be used for extending the solution in the outer layers.

At the base of the convective zone the potentials U_0, Q are discontinuous and vary on a scale short compared with the wavelength of an oscillation mode, Fig. 7 shows the variation of these potentials for model A. Here $\omega_0 = 0.0157$ Hz is a normalisation factor corresponding to $\nu = 2500\ \mu$Hz. We have superposed curves for $\nu = 1000, 2500, 4000\ \mu$Hz in Fig. 7; U_0 varies very slightly with frequency whilst $Q \propto \omega^{-2}$.

These sharp changes induce a periodic contribution $\Delta\delta_\ell$ to the phaseshifts, which can be obtained by integrating Eq. (22) over the discontinuity (cf. R&V 2001). The discontinuity can be approximately represented as

$$\Delta U_0 = \Delta U_\mathrm{D}\,\delta_D(t-t_1) + \Delta U_H\,H(t-t_1) \quad (24)$$
$$\Delta Q = \Delta Q_\mathrm{D}\,\delta_D(t-t_1) + \Delta Q_H\,H(t-t_1) \quad (25)$$

where $H(x)$ the Heaviside function with $\Delta U_H = U_0(t \gg t_1) - U_0(t \ll t_1)$, and $\delta_\mathrm{D}(x)$ the Dirac delta function with U_D the triangle shaped excess over the Heaviside function, and similarly for Q (cf. R&V 1994b). Note however that this is only a convenient approximation for simple analysis, it is actually the departure of U_0, Q from slowly varying functions over a wavelength that contributes to the seismic signature. On carrying out the integration of Eq. (23), (integrating the Heaviside component by parts) gives the result

$$\Delta\delta_\ell = (-1)^{\ell+1}\Big(K_1\sin(2[\omega t_1+\delta_\ell] - K_2\cos(2[\omega t_1+\delta_\ell])\Big) \quad (26)$$

where

$$K_1 = \left(\frac{\Delta V_\mathrm{H}}{4\omega^2} + \frac{\Delta Q_\mathrm{D}}{2}\right)\quad K_2 = \left(\frac{\Delta V_\mathrm{D}}{2\omega} - \frac{\Delta Q_\mathrm{H}}{4\omega}\right). \quad (27)$$

The periodic component of $\delta_1 - \delta_0$ is therefore

$$\Delta(\delta_1-\delta_0) = 2K_1\sin[2\omega t_1+\delta_0+\delta_1] - 2K_2\cos[2\omega t_1+\delta_0+\delta_1] \quad (28)$$

where we have taken $\cos(\delta_1 - \delta_0) \approx 1$ since $(\delta_1 - \delta_0) \sim 0.1$ (cf. Fig. 5). Since the base of the convective envelope is at 1422 s, we might expect the modulation period to be at ~352 μHz. But this is not so as the term $\delta_1 + \delta_0$ is frequency dependent and contributes the the modulation period. so too do the frequency dependent amplitudes.

A simple illustration of this is to take the function is

$$f(\nu) = \frac{1}{\nu*^2}\sin\left(\frac{2\pi\nu}{\nu_0} + \delta_1 + \delta_0\right) \quad (29)$$

(where $\nu* = \nu/2500$) in the frequency range $1000 \le \nu \le 4000$ with $\nu_0 = 351.6$ and $\delta_1 + \delta_0$ as shown in Fig. 5b. The Fourier power spectrum of this function is shown in Fig. 8. It has a maximum at a modulation period of ~359 μHz.

8. Analysis of solar data

The behaviour of the small separations $\nu^* dd_{01}, \nu^* dd_{10}$ for data from the BiSoN, IRIS, and the GOLF experiment on SoHO were shown in Fig. 2, they all show a behaviour similar to each other, and similar to that of the theoretical model.

To determine the phase shift differences and resulting power spectra for the modulation period we follow the analysis given in Sect. 6. We use the same frequency range for all data sets confining the analysis to modes of radial order $n = 9$ to 24 where the estimated 1σ errors on the frequencies are less than 0.1 μHz. The resulting values for the phase shift differences $\nu^*(\delta_1 - \delta_0)$ are shown in the top 4 panels of Fig. 9. Note that a 1σ error of 0.1 μHz in the frequencies translates into a 1σ error of 0.002 in $\delta_1 - \delta_0$. We then remove the mean trend by a low order fit as in Eq. (4) and take a power spectrum of the residuals to estimate the modulation period. The results for this frequency range are shown in the bottom panel of Fig. 9, giving the peak in the power spectra at 358 μHz (Bison), 359 μHz (IRIS), 359 μHz (GOLF) and 360 μHz (model A). There is reasonable agreement between the model and data sets.

Next we undertook a Mont-Carlo simulation with 10 000 random realisations of the errors - that is the frequencies were taken as $\nu_{n,\ell} + r_k\sigma_{n,\ell}$ with r_k generated by a random number generator with standard deviation 1 and a Gaussian distribution. This gave the following results for the mean peak modulation period and 1σ standard deviation:

BiSON : 358.2 ± 4.4, GOLF : 359.2 ± 6.8
IRIS : 358.7 ± 4.2, Model A : 359.7.

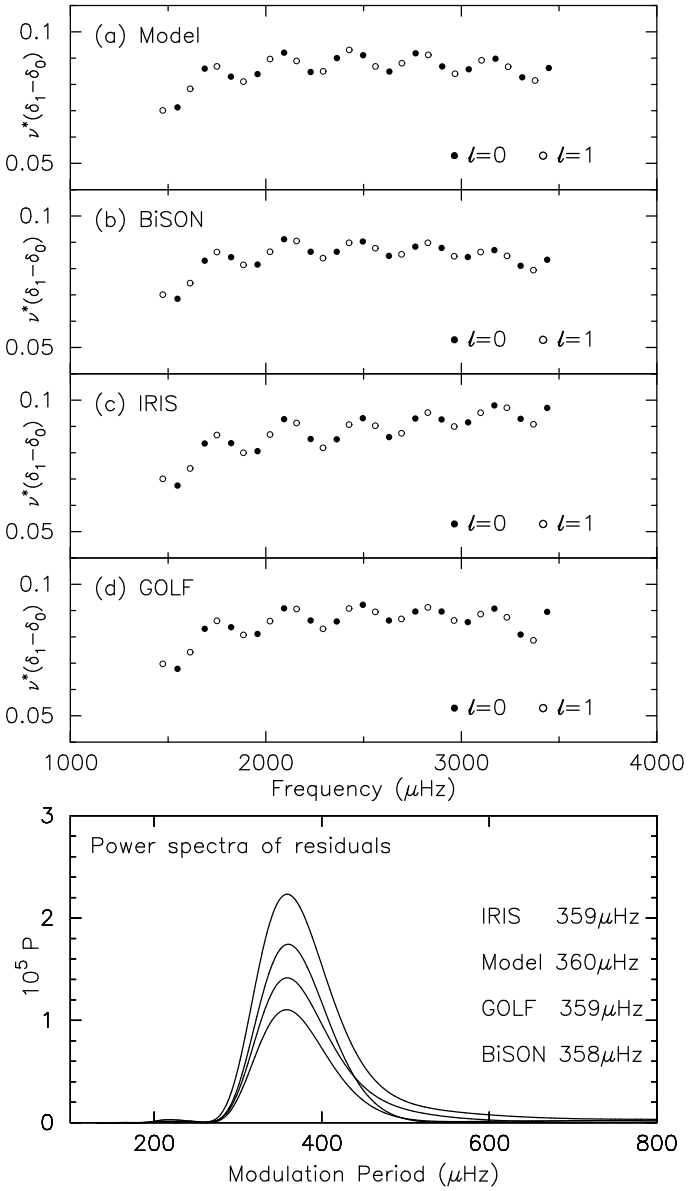

Fig. 9. $\nu^*(\delta_1 - \delta_0)$ derived from the frequencies as described in Sect. 6 for **a)** model A, **b)** a BiSON data set, **c)** IRIS data set, **d)** GOLF data set. All data sets were analysed using frequencies in the range 1400–3500 μHz. *Bottom panel*: power spectra of residuals to a low order fit as in Eq. (4). The modulation period at the peak of the power spectra are as listed. There is good agreement between the values derived from solar data and that of the model.

These are all in good agreement with each other – but indicate that the 1σ uncertainty in determining the modulation period ~4 μHz for the 11 year runs and ~7 μHz for the 2.2 year run with GOLF. These translate into an 1σ uncertainty in the acoustic radius of the base of the convective zone of ~20 s for the 11 year runs and ~30 s for the 2.2 year run.

However as shown above the modulation period is not simply $1/(2t_1)$ but is enhanced by ~6–7 μHz due to the frequency dependence of the phase shifts and the amplitudes of the oscillating signal. One might try to fit a model function to the data to determine these contributions at the same time as determining the frequency corresponding to the base of the convective zone (cf. Verner et al. 2004), but this depends on having a reliable parameterised model of the region below the base of the convective zone and of the internal phase shift difference. We will return to this matter in a subsequent paper where we also search for solar cycle variations.

9. Discussion

We have show that the periodicity in the small separations of p-modes of degree $\ell = 0, 1$ is due to the region of sharp change in acoustic variables at the base of the convective envelope, the modulation period being primarily determined by the *acoustic radius* t_1 of this interface. These separations are determined by the difference $\delta_1 - \delta_0$ between the internal phase shifts of modes of degree $\ell = 0, 1$. This phase shift difference can be directly derived from the frequencies using the Eigenfrequency equation. The modulation period is not precisely $1/(2t_1)$ as the peak frequency is modified by the frequency dependence of the phase shifts δ_0, δ_1, and by the frequency dependence of the amplitudes of the resulting signal. This periodic signal is not seen in small separations of modes of degree $\ell, \ell + 2$. This is because modes with degree differing by 2 are almost in phase when they reach the base of the convective zone whereas modes differing by 1 in degree are almost π out of phase. Other odd separations of modes of degree $\ell, \ell + 1$ will display a similar periodicity.

We have not so far considered the diagnostic value of the combination $\alpha - \delta_0$ which is directly calculated at eigenfrequencies $\nu_{n,0}$ and is known at $\nu_{n,1}$ once $\delta_1 - \delta_0$ has been calculated by interpolation at $\nu_{n,1}$ simply by adding $\delta_1 - \delta_0$ to $\alpha - \delta_1$. Even though α and δ_0 cannot be separately determined the combination $\alpha - \delta_0$ will nevertheless contain the signature of the HeII ionisation which can be extracted by a variety of procedures (cf. Brodskii & Vorontsov 1989; Vorontsov & Zharkov 1989; Gough 1990; Lopes et al. 1997; Perez-Hernandez & Christensen-Dalsgaard 1998; Roxburgh & Vorontsov 2001; Verner 2004) and used to infer the Helium abundance and entropy of the convective envelope.

Since the mean variation of $\delta_1 - \delta_0$ with frequency is determined by the structure of the inner regions of a star it provides a diagnostic of the internal structure; this can be used as the basis of crude inversion procedure to probe the internal density distribution by parameterising the structure in terms of values of the polytropic index at a few interior points (cf. Roxburgh 2000; R&V 2002), even when one only has data on $\ell = 0, 1$ modes. Moreover as shown by R&V (2003b) the requirement that the ℓ-dependent inner phase shifts δ_ℓ must match on to an ℓ-independent surface phase shift α can be used to find a best fit interior model out of a set of such models, independent of the structure of the surface layers, even when one only has modes with $\ell = 0, 1$ (R&V 2003b). The mean values of the small separation d_{01} and large separations, and their ratios, can be used with a 0, 1 asteroseismic diagram to place constraints on a possible stellar model (Christensen-Dalsgaard 1988; Mazumdar & Roxburgh 1993). Of course one can do better when one also has modes of higher degree, but as remarked at the beginning of this paper, for some stars we may only be able to detect modes of degree $\ell = 0, 1$.

Acknowledgements. I thank Graham Verner and the BiSON network for providing the 11 year frequency set used in the analysis, and the UK Science and Technology Facilities Council (STFC) which supported this work under grants PPA/G/S/2003/00137 and PP/E001793/1.

References

Brodskii, M. A., & Vorontsov, S. V. 1989, Ast Zh, 15, 69
Chaplin, W. J., Elsworth, Y., Miller, B. A., Verner, G. A., & New, R. 2007, ApJ, 659, 1749

Christensen-Dalsgaard, J. 1984, in Space Research Prospects in Stellar Activity and Variability, ed. A. Mangeney, & F. Praderie (Paris Observatory Press), 11
Christensen-Dalsgaard, J. 1988, in Advances in Helio and Asteroseismology, ed. J. Christensen-Dalsgaard, & S. Fransden (Reidel), 295
Christensen-Dalsgaard, J., Gough, D. O., Kosovichev, A. G., et al. 1996, Science, 272, 1296
Fossat, E., Salabert, D., & the IRIS group 2003, Proc. of the SOHO12/GONG+ 2002 Workshop, Local and global helioseismology: the present and future, ESA SP-517, 139
Gelly, B., Lazrek, M., Grec, G., et al. 2002, A&A, 394, 285
Gough D. O. 1983, Proceedings ESO Workshop on Primordial Helium, ed. P. A., Schaver , D., Knuth, & K., Kjar (Garching: ESO), 117
Gough, D. O. 1990, in Progress in Seismology of the Sun and Stars, ed. Y. Osaki, & H. Shibahashi, Lecture Notes in Physics (Berlin: Springer), 367, 283
Lopes, I., Turck-Chieze, S., Michel, E., & Goupil, M.-J. 1997, ApJ, 480, 794
Mazumdar, A., & Roxburgh, I. W. 2003, Asteroseismology Across the H.-R. Diagram, ed. M., Thompson, M., Cunha, & M., Monteiro (Kluwer Academic Publishers), 477
Montero, M., Christensen-Dalsgaard, J., & Thompson, M. 1994, A&A, 283, 274
Perez-Hernandez, F., & Christensen-Dalsgaard, J. 1998, MNRAS, 295, 344
Provost, J. 1983, Observational Tests of the Stellar Evolution Theory, ed. A., Maeder, & A., Renzini (Dordecht: Reidel), IAU Symp, 105, 47
Roxburgh, I. W. 1993, in PRISMA, Report of Phase A Study, ed. T., Appourchaux, et al., ESA SCI, 93, 31
Roxburgh, I. W. 2000, in Eddington, Assessment study Report, ed. F., Favata, I. W., Roxburgh, & Christensen-Dalsgaard, J., ESA-SCI, 8, Appendix A2, 103
Roxburgh, I. W. 2002, Proceedings of the First Eddington Workshop, ed. F., Favata, I. W., Roxburgh, & D., Galadi, ESA SP-485, 75
Roxburgh, I. W., & Vorontsov, S. V. 1994a, MNRAS, 267, 297
Roxburgh, I. W., & Vorontsov, S. V. 1994b, MNRAS, 268, 880
Roxburgh, I. W., & Vorontsov, S. V. 1996, MNRAS, 278, 940
Roxburgh, I. W., & Vorontsov, S. V. 2000, MNRAS, 317, 141
Roxburgh, I. W., & Vorontsov, S. V. 2001, MNRAS, 322, 85
Roxburgh, I. W., & Vorontsov, S. V. 2002, ESA SP-485, 341
Roxburgh, I. W., & Vorontsov, S. V. 2003a, A&A, 411, 215
Roxburgh, I. W., & Vorontsov, S. V. 2003b, Ap&SS, 284, 187
Tassoul, M. 1980, ApJS, 43, 469
Ulrich, R. K. 1986, ApJ, 306, L37
Unno, W., Osaki, Y., Ando, H., & Shibahashi, H. 1979, Nonradial Oscillations of Stars (Tokyo: Univ of Tokyo Press)
Verner, G. A. 2004, MNRAS, 351, 311
Verner, G. A. 2008, private communication
Vorontsov, S. V. 1988, in Advances in Helio- and Asteroseismology, ed. J. Christensen-Dalsgaard, & S. Fransden (Reidel), IAU Symp, 123, 151
Vorontsov, S. V., & Zarkhov, V. N. 1989, Astrophys. Space Sci. Rev., 7, 1